Cosmic γ-spectroscopy

I. L. Rozental', V. V. Usov, and I. V. Éstulin

Space Research Institute of the Academy of Sciences of the USSR
Usp. Fiz. Nauk **127**, 135–161 (January 1979)

Features of the origin of γ-lines under cosmic conditions, the methodology of cosmic γ-spectroscopy, and the characteristics of γ-spectrometers are discussed. Observational data are provided on discrete γ-lines caused by solar flares as well as on those arising in cosmic objects outside the solar system. A possible interpretation of the detected γ-lines is discussed. In closing the article, the prospects of cosmic γ-spectroscopy are analyzed.

PACS numbers: 94.40.Lx, 95.75.Fg, 95.85.Qx, 94.40.Cn

CONTENTS

1. Introduction 46
2. Features of nuclear reactions under cosmic conditions 46
   a) Nuclear γ-spectroscopy 46
   b) General considerations on the intensity of nuclear cosmic γ-lines 48
   c) On the profile of γ-lines 49
   d) Production of neutrons 50
   e) The annihilation γ-line 50
3. Methodology of cosmic γ-spectroscopy 51
4. Fundamental observational data 53
5. Astrophysical interpretation of the observational data 55
   a) γ-Lines from the Sun 55
   b) Galactic γ-lines 57
   c) γ-Lines from the radio galaxy Cen A 58
6. Results and future prospects 58
References 59

1. INTRODUCTION

Cosmic γ-spectroscopy is a new field of extraatmospheric astronomy. It is based on observing the line spectra of γ-quanta of energies ~10^{-1}–10 MeV that arise in outer space.[1)] These lines are due to annihilation of positrons and to nuclear reactions that occur in the outer layers of cosmic objects or in interstellar and intergalactic space.

The use of nuclear fusion reactions inside stars for interpreting their evolution has become customary for astrophysicists and needs no comment. In cosmic γ-spectroscopy we encounter new (for astronomers) physical phenomena and new (for physicists) objects of study.

Cosmic γ-spectroscopy helps us to study the properties of the outer layers of non-steady-state objects. Although the periods of existence of cosmic objects in a non-steady phase can differ substantially (from 1 sec to 10^{13} sec), yet they all have one extremely important feature in common: the existence of high-power fluxes of corpuscular particles of relatively high energies ($\gtrsim$0.1 MeV). Study of the characteristics of these fluxes is also facilitated by cosmic γ-spectroscopy.

It is now customary to bring together quite different fields of science "under one roof." However, when such a new science is in the process of being established, it takes a special approach to present it. One must satisfy the interests and curiosity of all the "interested parties"—in this case, the astrophysicists and nuclear physicists. Therefore some sections of our article (e.g., Sec. II) contain no substantially new information for specialists in the field of nuclear physics, while some other sections (Sec. V) are not very new for astrophysicists; however, as we see it, such extravagances are needed for a full understanding of the results and prospects of cosmic γ-spectroscopy by both physicists and astronomers.

2. FEATURES OF NUCLEAR REACTIONS UNDER COSMIC CONDITIONS

a) Nuclear γ-spectroscopy

The atomic nucleus is a complex quantum system having many discrete excitation levels. The energy difference between the levels is ~$2\hbar^2/m_p R^2 \approx 1$–10 MeV, where m_p is the mass of a proton, while $R \approx (0.3–1) \times 10^{-12}$ cm is the characteristic radius of nuclei. If we impart a large enough energy to an atomic nucleus during collision, then it will go into an excited state. Then after some time the nucleus will revert to the ground state or transform into other nuclei, thereby emitting nucleons, α-particles, $\beta^{\pm}$ electrons, or γ-quanta. We shall be interested below in the latter type of reaction, since only radiation is the direct source of information on cosmic objects.

We note two important properties of radiative transitions:

[1)] We note that studies of continuous cosmic γ-rays of quantum energy in the range 0.1–10^7 MeV (see, e.g., the review of Ref. 1) have also been developing very vigorously in recent years.

 0038-5670/79/010046-15$01.10

1) if the nucleus emits a γ-quantum after it has stopped, then the energy of the γ-quantum is E_γ = const within the accuracy of the natural line width ΔE_γ;

2) the natural line widths differ quite substantially from one another.

In the absence of competing processes, the lifetime $\Delta\tau_\gamma$ with respect to emitting a γ-quantum is connected to ΔE_γ by the uncertainty relationship

$$\Delta\tau_\gamma \cdot \Delta E_\gamma \sim \hbar. \tag{1}$$

If $\Delta\tau_\gamma \sim 10^{-17}$ sec, then we have $\Delta E_\gamma \sim 1$ keV.

The quantity $\Delta\tau_\gamma$ fluctuates considerably. As a rule it is small, though occasionally states are found with relatively long lifetimes. For example,[2] the line E_γ = 6.13 MeV in the spectrum of the ^{16}O nucleus has the lifetime $\Delta\tau_\gamma \sim 10^{-11}$ sec.

Usually the excited nuclei arise in a state of motion, and the Doppler effect gives rise to a shift (with directed motion of the nuclei) or a broadening (with random motion of the nuclei) of the γ-lines that they emit. An exception arises in the levels that emit during exceptionally long times in condensed media in which the nucleus can stop before decaying. Under cosmic conditions a nucleus practically always (with the possible exclusion of the dense photosphere of pulsars) emits while having the momentum that it received at the moment of excitation.

Let us examine further some possible types of excitation reactions of nuclei.

In the collision of electrons or positrons with nuclei, the interaction arises from electromagnetic forces:

$$e + (z,\ A) \to (z,\ A)^* + e'. \tag{2}$$

Here (z,A) is a nucleus of atomic number z and mass number A; and $(z,A)^*$ is the excited nucleus. Subsequently the nucleus $(z,A)^*$ can emit a γ-quantum in a transition to another state: $(z,A)^* \to (z,A) + \gamma$. As a rule, the most intense γ-lines correspond to transitions to the ground state.

The interaction of heavy charged particles (protons, α-particles, etc.) with the nuclei of the medium arises from electromagnetic and nuclear forces. An example of such a reaction is:

$$p + (z,\ A) \to (z,\ A)^* + p'. \tag{3}$$

Proton-capture reactions are also possible:

$$p + (z,\ A) \to (z+1,\ A+1)^* \tag{3a}$$

or ejection of a nucleon:

$$p + (z,\ A) \to (z-1,\ A-1)^* + 2p'. \tag{3b}$$

Figure 1 shows a diagram of the proton-capture reaction (3a).

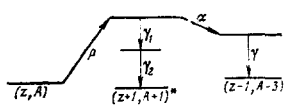

FIG. 1. Diagram of proton-capture reaction with production of the compound nucleus $(Z+1,\ A+1)$ and subsequent emission of α-particles and γ-quanta.

Moreover, nuclei can be excited in reactions involving neutrons. For example, we have:

$$n + (z,\ A) \to (z,\ A+1)^*, \tag{4}$$

$$n + (z,\ A) \to (z,\ A)^* + n', \tag{4a}$$

etc.

Reactions can also occur with breakdown of a target nucleus into two or more fragments that subsequently emit γ-quanta. For example, we have

$$p + (z,\ A) \to (z+1,\ A+1) \to (z_1,\ A_1) + (z_2,\ A_2). \tag{5}$$

Under cosmic conditions processes involving protons play the major role. This involves the following properties of the relativistic cosmic plasma:

a) it is electrically neutral;

b) very light nuclei and protons predominate in it.

This implies that the numbers of electrons and of heavy particles in the cosmic plasma are about the same. However, since the electromagnetic interaction constant is about 100 times smaller than that of the strong interaction, process (2), in which the electromagnetic forces dominate, is substantially suppressed as compared with reaction (3). Hence we can neglect process (2) in estimating the intensity of cosmic γ-lines.

The relative abundances of the elements in the universe and in cosmic rays differ only slightly from one another (a small enrichment of cosmic rays in complex nuclei is observed). The exceptions are the nuclei of Li, Be, and B, of which the cosmic rays contain about 10^5 times more than on the average over the universe. As we know, the abundance of the elements up to iron declines with increasing z. This implies that reaction (5) is less probable than reaction (3), if an excited nucleus is produced that has z and A values that coincide with those of the primary nucleus.

The excited states of Be and B can constitute exceptions, since a reaction of type (3) is improbable owing to the relatively low abundance of Li nuclei. Reaction (4) involving neutrons can be inefficient owing to decay of the neutrons (the half-life of neutrons is $\tau_n \sim 1000$ sec). In order for this reaction to proceed intensively, a high enough concentration n is required:

$$\sigma_{n\gamma} v \tau_n \gg 1. \tag{6}$$

Here $\sigma_{n\gamma}$ is the cross-section for the interaction of neutrons with nuclei accompanied by emission of γ-quanta, and v is the relative velocity of the neutrons and nuclei.

The cross-section for the reactions (4) involving neutrons is determined by the well-known Breit-Wigner formula. However, for rough estimates we can assume that

$$\sigma_{n\gamma} \sim \lambda^2. \tag{7}$$

Here λ is the wavelength of the neutron that corresponds to the resonance value E_γ. For estimates we can assume E_γ to be 10 MeV. Then Eq. (6) implies that

$n>10^{13}$ cm^3. We stress that this condition is necessary but not sufficient for the existence of intense cosmic rays emitted by excited nuclei produced by neutron capture. The existence of such γ-lines requires also powerful sources of neutrons, which themselves arise in nuclear reactions: e.g., of the type of (5) (for more details, see Sec. V). For all these reasons, the production of γ-lines in reactions (3) initiated by protons is more probable than in reactions (4) involving neutrons.

b) General considerations on the intensity of nuclear cosmic γ-lines

Let us find the general expressions for the luminosity in a given γ-line. We define the quantity q_α as follows: Let there be one nucleus per unit volume and let the concentration of cosmic protons having energies above E also be unity. Then the luminosity q_α in the given line $E_{\gamma\alpha}$ is the number of γ-quanta of this energy emitted per unit time.

Let us study the reaction (3) further. Let $\Psi(E)$ be the normalized differential spectrum of the protons in the cosmic rays:

$$\int_0^\infty \Psi(E)\,dE = 1. \tag{8}$$

Here E is the kinetic energy of the protons. We denote by ${}_zK^A$ the ratio of the concentration of the element of charge z and atomic weight A to the concentration of hydrogen. Then we have

$$q_\alpha = {}_zK^A \int_0^\infty \Psi(E)\,\sigma_\alpha(E)\,v_K\,dE. \tag{9}$$

Here $\sigma_\alpha(E)$ is the excitation cross section of the given level, and $v_K \approx \sqrt{2E/m_p}$. We are using the nonrelativistic approximation, since the main contribution to the integral in (9) comes from particles of energies $E \lesssim 100$ MeV.

Figure 2 shows the $\sigma(E)$ relationship for excitation of ^{12}C nuclei (with emission of the γ-line $E_\gamma = 4.43$) and of ^{16}O nuclei (γ-line 6.14 MeV) by protons and α-particles [$(p,p'\gamma)$ and $(\alpha,\alpha'\gamma)$ processes].

Table I gives the cross sections of certain reactions (see, e.g., Ref. 3).

The yield of γ-quanta in various reactions of particles having $E \sim 3$–10 MeV has been studied in many papers in connection with astrophysical applications. For example, $(p,p'\gamma)$ reactions of the nuclei ^{12}C, ^{28}Si, ^{29}Si, ^{46}Ti, ^{56}Fe, and ^{58}Ni have been studied in Refs. 4–8. The yield cross sections agreed in order of magnitude with the theoretical estimates made using the optical model.[9]

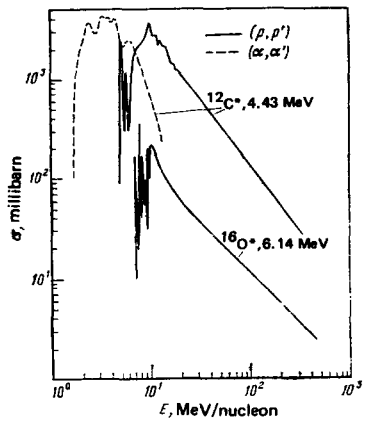

FIG. 2. Variation of the cross-section of *C* and *O* nuclei for excitation by protons and α-particles.

TABLE I

Nucleus	Energy of level, MeV	Value of cross-section, millibarns			
C^{12}	12.7	10 (18)	30 (20)	4 (28)	4 (30)
N^{14}	2.31	24 (8)	32 (10)	34 (14)	
	3.95	58 (8)	77 (10)	22 (14)	
O^{16}	6.92+7.12	80 (13)	70 (14)	55 (16)	40 (19)
	8.87			40 (16)	30 (19)
Si^{28}	1.37	320 (8)	150 (14)		
	1.78	320 (8)	150 (14)		
S^{32}	2.14	250 (5)	120 (8)	100 (11)	60 (14)

The values given in parentheses are the energies of the incident proton measured in MeV.

We can draw a number of important conclusions from Fig. 2 as well as Table I:

1. If the mass of the incident particle is substantially smaller than the mass of the particle at rest, then the cross-section $\sigma(E)$ has a maximum at $E \sim (2$–$4)E_\gamma$, and then it declines.

2. The cross-section approaches zero when the energy $E < 2E_\gamma$.

3. The $\sigma(E)$ relationship has a highly complicated form that is hard to represent analytically (especially in the region of the maximum).

4. Although the cross-section $\sigma(E)$ of different processes differ among themselves rather strongly, yet in the region of the maximum they are of the order of ~100 millibarn.

We can easily understand the first two of the listed properties on the basis of the laws of conservation of momentum, energy, and mass.

Let us study the collision of the nucleus (z_1, A_1) with the nucleus (z_2, A_2) at rest, with production of the compound nucleus (z_1+z_2, A_1+A_2). The reactions (3)–(5) are special cases of this more general reaction. In order that the compound nucleus (z_1+z_2, A_1+A_2) being produced can emit a quantum of energy E_γ, the mass of the compound nucleus must satisfy the condition

$${}_{z_1+z_2}M^{A_1+A_2} \geqslant {}_{z_1}M^{A_1} + {}_{z_2}M^{A_2} + E_\gamma. \tag{10}$$

In the nonrelativistic approximation this implies that the momentum p_{z_1} of the incident particle must satisfy the condition

$$\frac{p_{z_1}^2}{2}\left(\frac{1}{{}_{z_1}M^{A_1}} + \frac{1}{{}_{z_1}M^{A_1} + {}_{z_2}M^{A_2}}\right) \geqslant E_\gamma. \tag{11}$$

In other words, the energy threshold E_{thr} of the reaction satisfies in order of magnitude the conditions $E \gtrsim E_\gamma$ (for ${}_{z_1}M^{A_1} \ll {}_{z_2}M^{A_2}$) or $E_{\text{thr}} \gtrsim 2E_\gamma$ (for ${}_{z_1}M^{A_1} \sim {}_{z_2}M^{A_2}$).

The Coulomb barrier plays an essential role in depressing the reaction cross section of charged particles at low energies. The energy of the barrier is $E_b \sim z_1 z_2 e^2/R$ ($R \sim 10^{-12}$ cm is the characteristic dimension

of nuclei). For light nuclei E_b is about 10 MeV. The probability of reactions for $E<E_b$ (sub-barrier reactions) declines rapidly with decreasing energy E of the incident particle. Since the reaction cross sections in the immediate vicinity of the energy threshold are usually small (owing to the effect of the phase volume), then $\sigma(E)$ also rises with increasing E. However, then the resonance factor begins to operate. The latter arises from the discreteness of the levels, whereby the cross-section $\sigma(E)$ for $E \gtrsim (2-4)E_\gamma$ begins to decline with increasing energy E. The above-listed features of the behavior of the cross-section $\sigma(E)$ allow one to simplify substantially the calculation of the integral q_α in Eq. (9).

Usually the spectrum of the subcosmic rays is approximated as follows:

$$\Psi(E) = K_1 E^{-s} \quad \text{(nonthermal spectrum)}, \tag{12}$$

$$\Psi(E) = K_2 e^{-P/P_0} \quad \text{(quasithermal spectrum)}. \tag{13}$$

Here s, K_1, K_2, and P_0 are constants, E is the energy of the nucleus per nucleon, and P is the rigidity (momentum per unit charge).

Since the cosmic-ray spectrum declines rapidly with increasing E, we can substitute for E in the integral of (9) the value $E_{\max}$ at which the cross section $\sigma(E)$ reaches a maximum. In this case, taking $\Psi(E)$ as defined by Eq. (12), we have

$$q_\alpha \approx {}_zK^A N(>E_{\max})\,\sigma(E_{\max})\,v_K(E_{\max}). \tag{14}$$

Here $N(>E_{\max}) = \int_{E_{\max}}^{\infty} \Psi(E)dE$ is the integral spectrum of the cosmic rays. Analogously we have for the spectrum of (13):

$$q'_\alpha \simeq K^A N(>P_{\max})\,\sigma(P_{\max})\,v_K(P_{\max}); \tag{15}$$

here $P_{\max}$ is the rigidity that corresponds to $E_{\max}$.

In the first approximation, the ratio of intensities of the lines α and β is q_α/q_β.

Study of such relationships is important for determining the spectra and intensities of cosmic rays in the energy region of the order of several tens of megaelectron-volts.

Thus far we have assumed that the cosmic-ray spectrum does not change in time. In the actual case in non-steady-state objects, the cosmic-ray spectra (12) and (13) are altered by interactions with the medium. These are primarily electromagnetic interactions caused by ionization losses.

Whenever these losses are not compensated by a corresponding acceleration and the mean free path for these interactions is substantially smaller than the mean free path for production of γ-lines, then commonly such a medium is termed thick. For a thick medium, one must account for the transformation of the cosmic-ray spectrum caused by the total losses

$$\frac{dE}{dx} = f(E). \tag{16}$$

Here $f(E)$ allows for the electromagnetic losses due to ionization and to nuclear interactions (including the production of γ-lines). Equation (16) has a definite solution $E(x)$. When $x=0$, the distribution function has the form (12) or (13). If we know the solution $E(x)$, we can easily reconstruct $\Psi(E, x)$. Employing this function and Eq. (9) or (14) and (15), we can find the number of γ-quanta produced by the cosmic rays.[4]

The total luminosity of a cosmic object in the γ-line α is

$$L_{\gamma\alpha} = q_\alpha V_\alpha n_1 n_2. \tag{17}$$

Here V_α is the effective volume of the emitting region, and n_1 and n_2 are the concentrations of the cosmic rays and of the particles of the plasma that participate in the reaction.

The flux $I_{\gamma\alpha}$ of detectable γ-quanta at the boundary of the earth's atmosphere is

$$I_{\gamma\alpha} = \frac{L_{\gamma\alpha}}{4\pi R^2}. \tag{18}$$

Here R is the distance to the object under observation.

c) On the profile of γ-lines

We mentioned earlier that the natural width of the lines is small ($\lesssim 1$ keV). However, there are a number of additional factors that broaden the observed γ-lines. The most trivial one is the poor resolution of the instruments (see Sec. III). In certain observations this resolution has amounted to several tens of keV. Moreover, γ-lines can become substantially broadened by the following factors: 1) motion of the colliding particles, which leads to Doppler broadening; 2) scattering of the γ-radiation of the lines. Let us examine both these phenomena.

1) *Doppler broadening.* As we mentioned above, the compound nucleus under cosmic conditions almost always emits photons while moving at the same velocity v that it had at its instant of origin:

$$v = \sqrt{\frac{2E}{z_1 M^{A_1}}}. \tag{19}$$

Hence the Doppler shift will be $\sim v/c \sim \sqrt{2E/(z_1 M^{A_1} c^2)}$. For exact calculation of the broadening, we must average the ratio v/c over the spectrum $\Psi(E)$ of the colliding particles. However, for estimates it suffices to use the value $E = E_{\max}$ that corresponds to the maximum cross-section. For example, when $E = 2E_\gamma \sim 10$ MeV and $A = 10$, the width of the γ-line caused by the Doppler effect amounts to $\sim(0.05-0.1)E_\gamma$. We note, since the angle of emergence of the γ-quanta from the compound nucleus (in a system of coordinates associated with the nucleus) does not depend on its direction of motion, that the Doppler broadening extends on both sides of the detected line, in the "red" and "violet" regions.

2) *Scattering of γ-quanta.* As a rule, Compton scattering diminishes the energy of γ-quanta. An exception is the case in which the concentration of relativistic electrons is high enough. The broadening caused by the Compton effect is insignificant whenever the effective thickness of the emitting region is considerably smaller than the mean free path of the γ-quantum with respect to the Compton effect. For $E_\gamma \gtrsim 1$ MeV, this mean free path is $\sim 100\,\mathrm{g \cdot cm^{-2}}$. In principle the Compton effect makes itself felt even during passage of γ-quanta

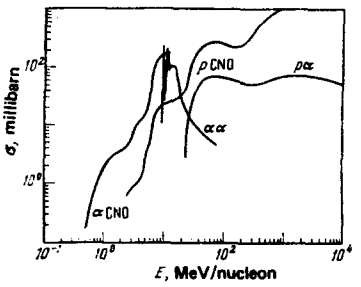

FIG. 3. Variation of the total cross-section for production of neutrons by protons in interactions with nuclei of light elements.[4]

through interstellar and interplanetary space. However, in this case the optical thickness is small—substantially smaller than $10\,g\cdot cm^{-2}$.

In the region of γ-quantum energies $E_\gamma \sim 1$–10 MeV, the Compton cross section declines, and hence the blurring of the γ-lines due to the Compton effect decreases with increasing E_γ.

In conclusion we note another exotic effect that leads to one-sided shift of γ-lines. If γ-quanta are emitted near a compact object (e.g., a neutron star), then a gravitational red shift occurs—a decrease in the energy of the γ-quanta when detected far from the object. For a neutron star this shift can be as much as ~10–20%.

d) Production of neutrons

Neutrons can arise in various nuclear reactions, e.g., in the reactions $^4He(\alpha, n)^7Be$; $^{12}C(p, pn)^{11}C$; $^{16}O(p, pn)^{15}O$, etc. They can also be produced in inelastic charge-exchange reactions, e.g.,

$$p + p \to p' + n + \pi^+. \tag{20}$$

Figure 3 shows the total cross sections for neutron production in the interaction of protons with light elements. Figure 4 gives the results of calculations[4] of the yield q_n of neutrons for a thin target in various reactions. Figures 3 and 4 imply that the charge-exchange reaction in the range of low neutron energies ($\lesssim$100 MeV) plays a substantially smaller role than the reactions involving complex nuclei. The total number of neutrons emitted per unit volume is $l_n = q_n n_1 n_2$, while the neutron flux within the limits of the emitting region is

$$I_n = l_n \tau_n \bar{v}_n. \tag{21}$$

Here $\bar{v}_n$ is the mean neutron velocity. The subsequent fate of the neutrons depends on the density of the medium. In a rarefied medium the neutrons will mainly decay. If the inequality (6) is satisfied, the fast neutrons produced in nuclear reactions can be slowed down to thermal velocities. Such thermal neutrons are mainly captured by protons: $n + p \to d + \gamma$. In this reaction $E_\gamma = 2.23$ MeV.

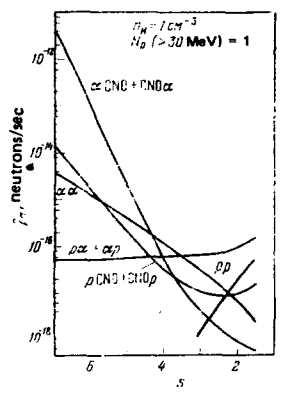

FIG. 4. Variation of the neutron yield q_n in a thin target when the spectrum of the incident particles follows a power law (s is the exponent of the energy spectrum).

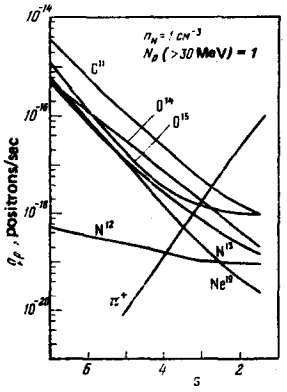

FIG. 5. Variation of the positron yield q_p in β^+-decays of nuclei excited by particles having a power-law spectrum (s is the exponent of the energy spectrum[4]).

e) The annihilation γ-line

Positrons can arise from the following processes: production of β^+-active nuclei (with subsequent decay) and production of π^+-mesons (with the subsequent decay $\pi^+ \to \mu^+ \to e^+$). Figure 5 shows the yield of positrons upon production of several unstable nuclei.

Positrons can also be produced in strong magnetic, electric, and gravitational fields.

The latter mechanism is especially nontrivial. It can occur only in the immediate vicinity of black holes of mass $M \lesssim 10^{17}$ g whose gravitational radius $2GM/c^2$ does not exceed $\sim\hbar/m_e c$ (see, e.g., Ref. 10).

In strong magnetic fields the following processes can occur:

$$\gamma + H \to H + e^+ + e^- \tag{22}$$

or

$$e^- + H \to H + 2e^- + e^+. \tag{23}$$

In an electric field e^+e^- pairs can be spontaneously created from the vacuum. This process occurs especially intensively when the electric field intensity $\mathscr{E}$ is close to the critical value $\mathscr{E}_{cr}$.

The critical field-intensity value $\mathscr{E}_{cr}$ is reached when the potential difference of the electric field multiplied by the charge of the electron reaches the value $m_e c^2$ of the mass of the field at a distance of the order of the Compton length $\hbar/m_e c$ of the electron. This yields the condition

$$\mathscr{E}_{cr} = \frac{m_e^2 c^3}{e\hbar} \sim 4\cdot 10^{13}\ \text{CGSE}. \tag{24}$$

Here e is the charge of the electron.

Such strong electric fields can exist only in the vicinity of extremely compact objects, e.g., pulsars.

When $\mathscr{E} \ll \mathscr{E}_{cr}$, the number of electron-positron pairs created per unit volume is

$$l_p = \frac{1}{4\pi}\left(\frac{e\mathscr{E}\hbar}{m_e^2 c^3}\right)^2 c \left(\frac{m_e c}{\hbar}\right)^4 \exp\left(-\frac{\pi m_e^2 c^3}{e\hbar\mathscr{E}}\right). \tag{25}$$

The process of e^+e^- pair production becomes rather efficient when $\mathscr{E} \sim 10^{11}-10^{12}$ CGSE.

If we use the customary formulas for magnetic bremsstrahlung (see, e.g., Ref. 11), then we can write the condition for efficient occurrence of process (23) in the form

$$\frac{eH\hbar}{m_e c}\left(\frac{E_e}{m_e c^2}\right)^2 \gtrsim m_e c^2. \tag{26}$$

From this we derive

$$H \geqslant \frac{m_e^2 c^3}{e\hbar}\left(\frac{m_e c^2}{E_e}\right)^2. \tag{27}$$

In this case the probability of pair production is $\sim\alpha\omega_{H\gamma}$ [$\omega_{H\gamma}$ is the probability of producing a photon with an energy determined by the condition (26); $\alpha = 1/137$ is the fine-structure constant].

Since positrons are annihilated mainly with emission of 2–3 quanta (see below), we can assume in estimates that the yield of annihilation γ-quanta is $I_\gamma \simeq q_\gamma n_1 n_2$. Here q_γ is the number of photons arising per unit volume per unit time when one positron and one electron exist per cm^3; n_1 and n_2 are the concentrations of electrons and positrons respectively.

This estimate holds when the mean free path of the positrons, which in our case is $\lesssim 1\ \mathrm{g\cdot cm^{-2}}$, is smaller than the dimensions of the emitting region.

Let us proceed to examine some details of the positron annihilation process.

Positrons can be annihilated either in the free state or in an already-bound state—positronium (Fig. 6). The cross section for two-photon annihilation σ_a as calculated by Dirac for

$$\gamma = \frac{\sqrt{E_p^2 + m_e^2 c^4}}{m_e c^2} \gg 1 \tag{28}$$

has the form

$$\sigma_a = \sigma_0 \frac{\ln \gamma}{\gamma}, \tag{29}$$

where we have

$$\sigma_0 = \pi\left(\frac{e^2}{m_e c^2}\right)^2 \approx 2\cdot 10^{-25}\ \mathrm{cm^{-2}}.$$

In the other important limiting case where $E_p \ll m_e c^2 (\gamma \sim 1)$, we have

$$\sigma_a \approx \sigma_0 \frac{c}{v_p}. \tag{30}$$

We note that free annihilation into n ($n>2$) photons is relatively improbable: $\sigma_a(n\gamma) \sim \sigma(2\gamma)\alpha^{n-2}$. Whenever positronium is formed, two states can exist: orthopositronium, which decays into three γ-quanta, and parapositronium, which decays into two γ-quanta.

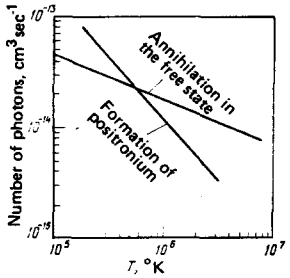

FIG. 6. Probability of annihilation in the free state and after formation of positronium.[4]

Decay into two quanta in the limiting case of (30) or in the parapositronium case leads (without accounting for possible broadening) to a distinct line of energy $E_\gamma = 0.51$ MeV. However, three-photon decay yields a diffuse spectrum with an energy in the range $0 < E_\gamma < 0.51$ MeV. Hence the resultant distribution of photons with respect to the energy E_γ depends on the fraction of orthopositronium decays, which in turn is determined by the parameters of the plasma. This problem has been treated in detail in Ref. 12. The qualitative conclusions derived in the study are highly perspicuous:

1) as the temperature approaches 10^5 °K, the role of three-photon decay increases, and the natural line width increases;

2) when $T \ll 10^5$ °K or $T \gg 10^5$ °K, the positron is annihilated with emission of the line $E_\gamma = 0.51$ MeV. The line width is determined by the lifetime and by Doppler broadening;

3) when three-photon decay plays a considerable role, the resolving power of the instrument plays a definite role. The mean energy of the detected annihilation γ-line is determined by averaging the spectrum over the resolution interval of the instrument.

In closing this section, let us examine the influence of other effects on the width of the annihilation γ-line. The natural width of the annihilation line is very small.[13] The broadening due to the Doppler effect is more substantial. Here we must distinguish two cases: 1) annihilation of positrons in flight, i.e., when $E_p \gg kT$, 2) annihilation of positrons having energies close to kT. If $E_p \lesssim 1$ MeV, then the probability of annihilation in flight is ~1%, and hence we can neglect it. However, if relativistic positrons are being produced with $E_p \gtrsim 10$ MeV, then their annihilation probability in the relativistic state increases and reaches 10%. As a rule, the broadening due to the thermal motion of e^+e^- pairs is quite substantial. The width of the annihilation γ-line amounts in order of magnitude to

$$\Delta E_\gamma \simeq 1.8\cdot 10^{-5} m_e c^2 \sqrt{T}. \tag{31}$$

Here T is the temperature of the plasma measured in °K.

Thus an exact study of the annihilation-line profile can enable one to determine the spectrum of subcosmic rays, and in the case of established thermal equilibrium—the temperature of the plasma.

3. METHODOLOGY OF COSMIC γ-SPECTROSCOPY

A cosmic γ-spectrometer consists of a spectrometric γ-ray detector and a multichannel amplitude analyzer. In most of the experimental studies discussed below, scintillation γ-detectors with NaI (Tl) crystals and analyzers with 128–512 channels have been used. In recent years Ge (Li) detectors and pulse analyzers with 4048 channels have begun to be used.

Cosmic γ-spectroscopy has its own methodological features, namely:

1) The Earth's atmosphere (of thickness ~1 kg/cm^2)

is opaque to the γ-rays in the range of interest to us. Hence one must either elevate apparatus for measuring cosmic γ-lines to the boundaries of the atmosphere (balloon experiments) or put them in a spacecraft. For example, in operating with a Ge (Li) detector in a spacecraft under conditions of weightlessness, the problem arises of designing a special cooling device.

2) In cosmic studies the discrete γ-lines are manifested against a background of continuous radiation of comparable intensity. Hence one must take measures to increase the ratio of the useful signal to background.

3) In studying cosmic objects, one must bear in mind the fact that the counts from the apparatus when observing the source do not exceed 10–20% of the count from background radiation. In balloon measurements, the background mainly involves atmospheric γ-rays that arise under the action of cosmic rays. In working in a spacecraft, the intrinsic emission of the latter can exceed by an order of magnitude the intensity of the diffuse cosmic radiation.[15] Moreover, γ-lines can exist in the background radiation, which hinders identifying them with a source. For example, the intensity of the γ-line of energy 511 keV in the background in cosmic studies amounts to no less than $\sim 5\times10^{-2}$ quanta/cm$^2\cdot$ sec, whereas the intensity of this γ-line from cosmic objects does not exceed the order of 10^{-3} quanta/cm$^2\cdot$ sec. Therefore one usually applies a difference method of spectral measurements in which one separately measures the background n_b and the radiation in the direction of the cosmic source n_γ. The sought radiation flux of the celestial source n_s is found by subtracting the spectra:

$$n_s = n_\gamma - n_b. \tag{32}$$

The difference method of measurements requires high stability of operation of the apparatus.

4) The intensities of cosmic γ-lines at the Earth as predicted in most theoretical studies lie at the level 10^{-5}–10^{-6} quanta/cm$^2\cdot$ sec. Fluxes have been found experimentally at the level of 10^{-4} and even 10^{-3} quanta/cm$^2\cdot$ sec. When one uses the difference method, prolonged observations are required for reliable detection of γ-lines of weak intensity from discrete sources. In balloon experiments the observation of a fixed celestial object has not exceeded four hours.[16] Only in spacecraft is it practical to make exposures in measurements of up to days or weeks.

Detectors of γ-rays with an angle of view of about 4π have been used in studying diffuse cosmic γ-rays.[15,17,19] In these experiments a γ-line of energy ~510 keV, was found, but difficulties arise in identifying the source, since difference measurements cannot be made. We note in principle two possibilities of making the measurements: in studying the Sun, to compare measurements made in the day or night,[20] and to compare measurements while the Earth is eclipsing particular regions of the sky[21] (e.g., the center of the Galaxy). These possibilities do not seem very promising to us, owing to the high background in a global detector. Studies of γ-lines using global detectors have been treated earlier by one of the authors of this article.[22] The cosmic nature of the γ-lines observed here was not reliably established, in spite of multiple repetition of the experiments.[23]

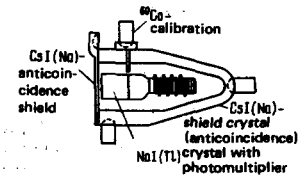

FIG. 7. γ-Ray spectrometer that operated in the OSO-7 satellite.

Reliable data on the intensities of cosmic γ-lines have been obtained by employing a spectrometric detector combined with a γ-ray collimator. Below we shall take up some concrete types of such instruments. The scientific results obtained by using these instruments are described in the following sections of this article.

Figure 7 shows a detector employed for seeking γ-lines in solar flares.[24,25] The γ-detecting NaI (Tl) crystal of effective area 45 cm^2 was placed together with a photomultiplier in a shell made of a CsI (Na) crystal. The angle of view of the instrument of 120° ×70° was shielded by a thin layer of CsI (Na) to exclude counting of charged particles in the central detector. The spectrometer measured radiation in the energy range from 0.3 to 9.1 MeV. The instrument operated in a rotating section of the OSO-7 satellite, and included a multichannel pulse analyzer having 377 channels. In flight the energy calibration of the spectrometer was performed with a radioactive ^{60}Co source.

A diagram of a typical γ-ray spectrometer employed in balloon experiments has been given in Ref. 26.

Figure 8 shows a setup with a Ge (Li) spectrometer and a system for cooling the detector[27] that operated on the polar satellite 1972-076 B. The detector of volume 50 cm^3 with an effective area $S=15$ cm^2 was shielded with a plastic scintillator of thickness about 30 g/cm^2. Radiation was detected with energies 0.04–2.7 MeV over the broad aperture angle $\varphi=\pm45°$. The energy resolution of the spectrometer in the first 10 days of flight was $\Delta E=3.5$–4 keV, while later it deteriorated to 10 keV owing to leakage of the bias voltage applied to the Ge (Li) detector. The axis of the instrument was

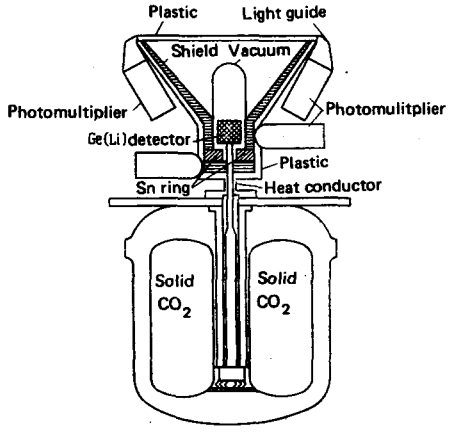

FIG. 8. Apparatus with a Ge(Li) detector that operated in the 1972-076 satellite.

scanned over the sky and the atmosphere of the Earth at the rate of one revolution per 5 sec. The cryogenic apparatus for cooling the detector was a cryostat with a solid CO_2 coolant (15 kg). The cryostat maintained a constant temperature of the detector $T = 130$ °K during 7–8 months of flight. The published data[28] give the energies of 20 different γ-lines and their interpretation as radiation of the atmosphere and the apparatus γ-lines of the detector. The latter arise mainly in processes of radiative neutron capture (n, γ) and subsequent activation of the detector. The astrophysical results of scanning the spectrometer over the celestial sphere[29] will be discussed in later sections of the article.

The instruments depicted in Figs. 7 and 8 employed a shield made of scintillators as the active collimator. The collimator has a multipurpose task. First, it limits the angle of view of the central detector. We note that considerable difficulties arise in designing a spectrometer having a small aperture angle ($\varphi < 10°$) for γ-rays of energies 0.5–5 MeV. Second, the active collimator discriminates against pulses from energetic charged particles, including those from γ-rays arising in the collimator upon reacting with energetic charged particles. The influence is also partially eliminated of the activation of the collimator, except for cases of excitation of isomeric nuclear states. Third, the collimator ensures operation of the central detector in a regime of suppressed Compton scattering.

We note that the resolution of a Ge (Li) spectrometer exceeds that of scintillation spectrometers by a factor of more than 15. Therefore Ge (Li) spectrometers are highly promising for further experiments. In particular, we should consider Ref. 27 as proving the possibility of prolonged operation of a Ge (Li) spectrometer under space conditions. However, a large number of apparatus γ-lines are found when one employs a spectrometer of high energy resolution (see, e.g., the above-cited Ref. 28). Many background γ-lines are also detected when a Ge (Li) detector is lifted in balloons.[30,31] Further methodological improvements in order to diminish the background lines and development of a method of revealing an effect against the "background" of the remaining γ-lines are needed.

4. FUNDAMENTAL OBSERVATIONAL DATA

In 1972 a large number of flares was observed on the Sun that were accompanied by emission of X- and γ-rays. For example, the high-apogee satellite "Prognoz-2" ($R_A \sim 200$ thousand km) detected 29 solar flares in the period from Apr. 14 to Aug. 1, 1972 with emission of hard X-rays in the region 30–350 keV.[32]

Intense emission of γ-lines was detected by the low-apogee satellite OSO-7 during the very large flares on the Sun on Aug. 2, 4, and 7 of 1972. Figure 9 shows the spectrum of the pulses measured during the solar flares of Aug. 4, 1972.[33] We clearly see peaks from γ-lines at energies of 0.5, 2.2, 4.4, and 6.1 MeV, as well as peaks from the calibration source.[25] The curve below is the background spectrum in simultaneous measurements in the antisolar direction.

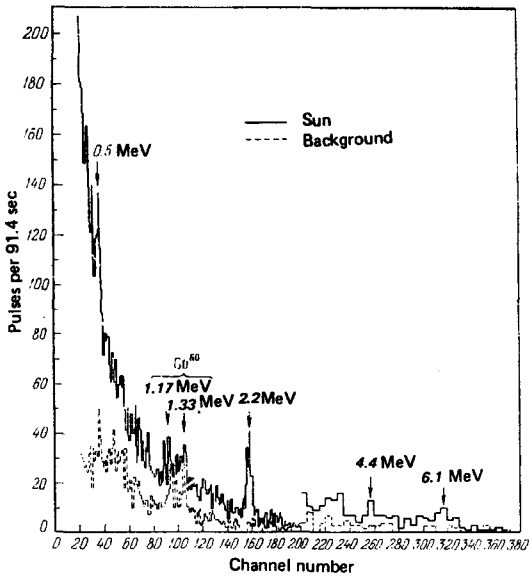

FIG. 9. Spectrum of pulses detected on Aug. 4, 1972 during a solar flare (6.26–6.35 AM).

Table II gives the experimental data on the γ-lines observed during the solar flares in August 1972. The third and fourth columns of the table are the data of Ref. 24. Here the mean fluxes of γ-quanta in the individual γ-lines (photons/cm^2·sec) are given as measured on Aug. 4 and 7 in a period of 9 minutes.

The time course of rise and decay of the γ-line of energy $E_\gamma = 2.2$ MeV is discussed in Ref. 34. These data are shown in Fig. 10.

Detection has been reported[35] of γ-lines by the satellite "Prognoz-2" during the solar flare of Aug. 2, 1972. The stilbene detecting crystal of the instrument did not allow discrimination of the peaks from the γ-lines and did not satisfy the original requirements for γ-spectroscopy (see Sec. 3). However, the radiation flux in the γ-line of energy $E_\gamma = 0.5$ MeV and an upper limit for $E_\gamma = 2.2$ MeV were determined from the shape of the γ-ray spectrum during the flare (2nd column of Table II).

Repeated attempts have been made to detect γ-lines from the quiet Sun.[23] The upper limits obtained on the radiation flux of γ-lines, e.g., from the data of Ref. 30, exceed the theoretical predictions by about two orders of magnitude.

Detection of a nuclear γ-line of cosmic origin was first reported in Refs. 26 and 37. In this experiment a spectrometer was employed having the following technical data: $S_{\text{eff}} = 75$ cm^2, angle of view $\phi = 24°$. The in-

TABLE II. Flux of γ-quanta (photons/cm^2·sec) in individual lines at the Earth during the solar flares in August 1972.

Energy E_γ, MeV	Time of measurement (date, August, 1972)		
	Aug. 2	Aug. 4	Aug. 7
	$20^h\ 46^m$	$06^h26^m - 06^h35^m$	$15^h38^m - 15^h47^m$
0.5	0.6 ± 0.5	$(7 \pm 1.5) \cdot 10^{-2}$	$(3.7 + 0.9) \cdot 10^{-2}$
2.2	< 0.33	$(2.2 \pm 0.2) \cdot 10^{-1}$	$(2.6 \pm 1) \cdot 10^{-2}$
4.4	—	$(3 \pm 1) \cdot 10^{-2}$	$< 2 \cdot 10^{-2}$
6.1	—	$(3 \pm 1) \cdot 10^{-2}$	$< 2 \cdot 10^{-2}$

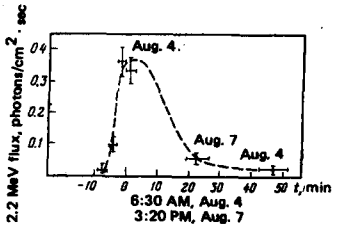

FIG. 10. Time dependence of the intensity of the γ-line $E_\gamma = 2.2$ MeV during the solar flares of August 1972.

strument was lifted in a balloon in 1970 to a height of residual atmosphere ~3.1–3.4 g/cm^2. An extra count of pulses was observed at the moment of passage through the region of the galactic center when the axis of the instrument coincided with the galactic X-ray source GX3+1. A peak was noted in the spectrum of the pulses from a γ-line of energy $E = 476 \pm 24$ keV. Data on the intensity of the γ-line and the shape of the continuous spectrum of the source as measured in the stated time interval are given in the second column of Table III.

The search for γ-lines has also been conducted in balloon experiments: on May 15, 1973,[38] and during the night from Apr. 1 to 2, 1974.[16] Figure 11 shows a map of the sky in galactic coordinates; the dots indicate x-ray sources according to the "Uhuru" catalog. The circles of diameter 15° indicate the regions of the sky observed on this flight, with centers at GX1+4[16] and Cen A ($\alpha = 13^h23^m$, $\delta = -42°53'$).[39]

In observing the region of the galactic center, the axis of the spectrometer was aligned in the direction of the x-ray source GX1+4. This region of the sky was

TABLE III

Direction of the axis of the instrument	Center of the Galaxy		$l^{II} = 345°$, $b^{II} = +35°$	Cen A	Crab Nebula	
	GX3+1	GX1+4				
Date of observations / Energy of γ-line, MeV	Nov. 25 1970	Apr. 1–2, 1974			May 15, 1973	May, 1976
0.400±0.001						(2.24 0.65) ×10^{-3}
0.476±0.024	(1.8 ±0.5)·10^{-3}					
0.53±0.01		(8 ±2.3)·10^{-4}	< 5·10^{-4}			
0.9±0.1		(3.7 ±3.1)·10^{-4}				
1.15±0.07			(3.4 ±1.5)·10^{-3}		< 10^{-3}	
1.6				(3.4 ±1.5)·10^{-3}		
1.2–2.0		(2.6 ±0.6)·10^{-3}				
4.6±0.1		(9.5 ±2.7)·10^{-4}		(9.9 ±3)·10^{-4}		
Flux of continuous radiation, quanta/cm^2 · sec · keV	(10.5±2.2 ×$E^{-2.3}$	(40.7 ±12.5) / $E^{-(2.78\pm0.6)}$	(9.5 ±2.6) × $E^{-(2.4\pm0.1)}$	(0.86 ±0.17) ×$E^{-(1.90\pm0.04)}$		
Distance to object, kpc	~ 10		~ 3	5·10^3	1.7	
Luminosity, erg/sec — Continuous radiation		1.3·10^{36}	6.5·10^{37}	4.7·10^{43}		
Luminosity, erg/sec — γ-Lines		10^{37}	7·10^{36} 7·10^{37}	2.6·10^{43} 2.2·10^{43}		4·10^{36}

The values given in the table of fluxes of γ-quanta in the lines are measured in quanta/cm^2 · sec.

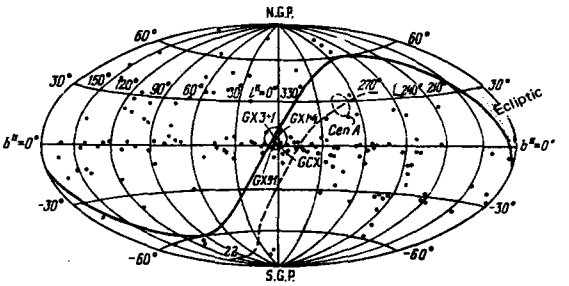

FIG. 11. Map of the sky in galactic coordinates.

followed for about 4 hours. Figure 12 shows the effect of the source with the background subtracted. The power law of the continuous spectrum of the emission of the source was determined from measurements at low energies $E_\gamma < 300$ keV. The form of the continuous spectrum found in Ref. 16 agrees with the measured intensities in the region $E_\gamma \gtrsim 100$ MeV from the data of the SAS-2 satellite. Figure 13 shows the spectrum in excess of the continuous distribution. The peaks from the γ-lines $E_\gamma = 530 \pm 10$ keV and 4.6 ± 0.1 MeV were found with a reliability of 3.6σ (from the area of the peaks). The intensities of the γ-lines are given below in Table III. It was not possible to resolve the region of the spectrum in the range 1.2–2 MeV into individual γ-lines. The peak of energy 0.9 ± 0.1 MeV is poorly marked.

It is natural to compare the results of studying the region of the galactic center in 1970[37] with the measurements of 1974[16] (see Table III). The existence of a γ-line of energy 476 keV was not confirmed in the repeat experiments. The authors of Ref. 16 point out a possible explanation in the differing angles of view of the spectrometers employed in Ref. 36 ($\varphi = 24°$) and Ref. 16 ($\varphi = 15°$). The line at $E_\gamma = 476$ keV may be emitted from the region of the galactic disk having coordinates $8° \lesssim l'' < 17°$, which was not studied in the 1974 measurements. Refs. 36 and 16 also differ in the results of measuring the intensity of the continuous radiation from the region of the galactic center (see Table III).

In comparing the results of measuring the background in different regions of the sky (dashed lines in Fig. 11) in sector 10, where the dotted curve crosses the galactic disk, they found an excess count.[40] In 30 minutes of

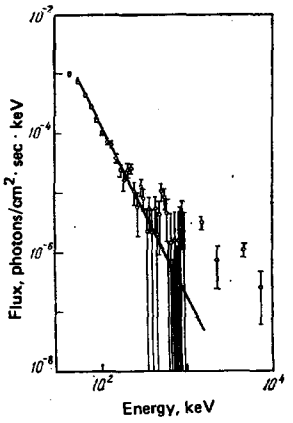

FIG. 12. γ-Ray spectrum detected in observing the galactic center. The straight line is the power law $40.7\ E^{-2.78}$.

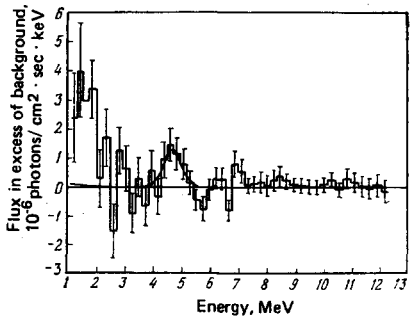

FIG. 13. Spectrum of the radiation in excess of the continuous background in measurements of the region of the galactic center.

observations, they found a continuous spectrum of the shape of $9.5E^{-2.4}$, the power law of which agrees with the data measured in the SAS-2 satellite for γ-quanta having $E_\gamma \gtrsim 100$ MeV. The resulting spectrum, or more exactly, the excess over the continuous distribution, was obtained upon observing a region of the Galaxy in the form of a circle of radius 6.5° with its center at the coordinates $l'' = 345°$, $b'' = +5°$. A peak stands out on the histogram at the energy 1.15 ± 0.07 MeV that exceeds the mean counting level by 2.6σ. An upper limit is also given[40] for the intensity of the γ-line at 0.5 MeV.

Figure 14 shows the excess over the continuous distribution in an observation of the region Cen A (the observations took 85 minutes).[39] We can see symmetric peaks at energies 1.6 and 4.5 MeV. Here the peak at energy 1.6 MeV is broadened by a factor of three times the apparatus width of the peak. The natural width of this peak is $\Delta E = 350$ keV (assuming it to be single). Yet we cannot rule out the more realistic assumption that the peak has a complex structure, i.e., consists of several γ-lines that are not resolved by the spectrometer. The peak width of the γ-line at 4.5 MeV does not exceed the apparatus width. In view of the remoteness of the object ($R = 5$ Mpc), the appreciable intensity of the γ-line at the Earth (see Table III) indicates a considerable luminosity of Cen A in these lines.

Three objects were observed during one of the balloon experiments: the Crab Nebula, the pulsar NP 0532, and the Perseus galaxy cluster.[38] In studying the Crab Nebula and the Perseus cluster a method of rotating the spectrometer was used to record the "background." In detecting the pulsar NP 0532, the pulses were classified in time into the pulsar-flash time (measuring the effect of the source) and the gaps (detecting

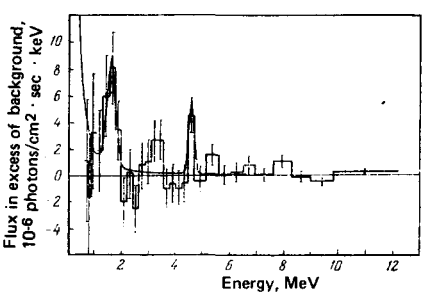

FIG. 14. Spectrum of γ-rays observed from Cen A.

the "background"). In all three cases emission from the studied objects was found in the form of a continuous spectral distribution without an excess from γ-lines. At the 2σ level upper limits were obtained on the radiation flux of γ-lines at the Earth of $I_\gamma < 10^{-3}$ photons/cm^2 · sec (see Table III).

Interesting results[41] have recently been obtained in observations employing a Ge (Li) spectrometer with a collimator made of NaI (Tl) on the Crab Nebula in a balloon experiment. Radiation was detected in the energy range 0.1–5 MeV in an aperture angle of the instrument of $\varphi = 11°$. One of the 12 γ-lines ($E_\gamma = 400 \pm 1$ keV) that had been observed in the spectrum by the difference method was assigned to a source in the region of the Crab Nebula. The broadening of this γ-line is $\lesssim 2$–3 keV, and the radiation flux at the Earth is $I_\gamma \simeq 10^{-3}$ photons/cm^2 · sec. However, difficulties arise in comparing the experimental data of Refs. 41 and 39, since, as was pointed out above, γ-lines having $I_\gamma > 10^{-3}$ photons/cm^2 · sec were not detected in Ref. 39.

The results of a 10-day scan of the sky with a Ge (Li) spectrometer (see Fig. 8) are given in Ref. 29. Analysis of the energy spectrum indicates emission from the region of galactic latitudes 255–328° of γ-lines of energies 1121 and 1369 keV. The authors of the experiment ascribe these γ-lines to processes of inelastic interaction of subcosmic rays with ^{48}Ti and ^{24}Mg nuclei, respectively.[42]

A report[43] has given the results of a balloon experiment performed in 1974 with a Ge (Li) spectrometer having an aperture angle of 30°. When a transient x-ray source that flared for 15 minutes passed into the field of view of the spectrometer γ-ray lines of 1.8 and 6.1 MeV were detected. The axis of the instrument at the instant of observing the γ-lines had the celestial coordinates $\alpha = 6^h 56^m$ and $\delta = 22°$. The radiation flux in the γ-lines, which apparently involved excited nuclei of ^{28}Si (1.8 MeV) and ^{16}O (6.1 Mev) was of the order of 10^{-6} erg/cm^2 · sec.

The experimental results discussed in this chapter are given in Table III, where the upper rows give the fluxes of the γ-lines at the Earth (photons/cm^2 · sec). The lower rows of the table contain certain supplementary data on the sources emitting the γ-lines: the shape of the continuous-radiation spectrum measured at the instant of detecting the γ-lines, the distance R to the object, and the luminosity L_γ in the continuous spectrum and in the γ-lines. The distance $R = 3$ kpc for the region $l'' = 345°$, $b'' = +5°$ (4th column of the table) was obtained by assuming that the radiation of ^{44}Sc ($E_\gamma = 1.156$ MeV) is being detected; it is genetically associated with the decay of ^{44}Ti. The radioactive isotope ^{44}Ti is contained in the remnants from explosion of supernovas.

5. ASTROPHYSICAL INTERPRETATION OF THE OBSERVATIONAL DATA

a) γ-lines from the sun

As we mentioned in Sec. 4, γ-lines have been detected during solar flares with the quantum energies of 0.5, 2.2, 4.4, and 6.1 MeV. Let us examine the nature of

this radiation.

The 2-2 MeV line is emitted during formation of deuterium nuclei by capture of thermal neutrons by protons: $p+n\to d+\gamma$. The processes in which thermal neutrons are produced during solar flares are discussed in Sec. 2. An analysis of propagation of neutrons in the solar atmosphere and of generation of the 2.2-MeV γ-line has been carried out in Refs. 44–46. It was assumed that initially the neutrons are isotropically distributed in the chromosphere or in the lower corona, and then propagate independently of the magnetic field of the Sun and interact with the matter of its atmosphere. The fundamental processes of interaction of neutrons with the solar plasma are elastic scattering by protons and capture of neutrons by protons and He nuclei (see Sec. 2). The role of the other nuclei in neutron capture is small [e.g., the probability of the reaction $^{14}N(n,p)^{14}C$ constitutes less than 10^{-5} of the overall neutron-capture probability]. Only in capture of neutrons by protons are γ-quanta produced. The capture of a neutron by a ^{3}He nucleus occurs without emitting a γ-quantum.

The intensity of the 2.2-MeV γ-line depends very strongly on the ratio of concentrations of hydrogen and helium in the region of most efficient neutron capture. Even a very small helium content suffices to depress emission in the given γ-line. Actually, the capture cross-sections of neutrons by protons and helium nuclei are $2.2\times10^{-30}\beta^{-1}$ cm^2 and $3.7\times10^{-26}\beta^{-1}$ cm^2, respectively. Here $\beta=v/c$, while v is the velocity of the neutron with respect to the particle that captures it. Hence we see that the rates of capture of neutrons by protons and helium nuclei are equal when the ratio of concentrations of ^{3}He and ^{1}H amounts to $\sim6\times10^{-5}$. Thus, at a ^{3}He concentration outside the neutron-capture region [subphotospheric layers of density $\sim(1-3)\times10^{17}$ cm^{-3}] higher than $6\times10^{-5}N_H$, capture of neutrons by helium nuclei will predominate, and hence the intensity of the 2.2-MeV line will be depressed.

Let us estimate the radiation flux in the 2.2-MeV line. In order to do this, we shall employ the following formula for the value of the total γ-ray flux throughout a flare at the distance r from the Sun (see Sec. 2 and Ref. 47):

$$F_\gamma\simeq\frac{\varkappa}{4\pi r^2}\sum_{i=C,\,N,\,O}\frac{n_i}{n_H}\int_{E_{\text{threshold}}}W_{pi}\frac{X}{\lambda}N_p(E)\,dE. \tag{33}$$

Here $\varkappa$ is a coefficient that determines the fraction of the neutrons absorbed by hydrogen to form deuterium and emit a γ-quantum, n_i/n_H is the relative concentration of nuclei in the atmosphere of the Sun, $\lambda(E)$ is the mean free path of a proton for nuclear interaction with the nucleus i, $X(E)$ is the thickness of matter traversed by the accelerated particles, $N_p(E)$ is the differential spectrum of the total number of protons in the region of the flare, and W_{pi} is the probability that a γ-quantum will be produced by nuclear reaction of the proton with the nucleus i.

The mean thickness X of matter through which the accelerated particles pass until they emerge into the interplanetary medium apparently does not exceed several tens of milligrams,[48] i.e., we have $\lambda/X\approx2\times10^3$. This quantity is also of the same order of magnitude when the accelerated protons move in the direction toward the Sun, since the low-energy protons make the major contribution to the studied process.[47]

The fraction of neutrons absorbed by hydrogen in the atmosphere of the Sun depends on the abundance of ^{3}He. According to Ref. 4, it varies from 0.1 to 0.4. If we adopt for the sake of concreteness $\varkappa=0.2$, we get from (33) the following relationship between the total number of protons N_p^Σ that "settle" in the atmosphere of the Sun and the expected value of the total flux of γ-quanta per flare[47]:

$$F_\gamma\approx2\cdot10^{-34}N_p^\Sigma\qquad(E\geqslant2\text{ MeV}). \tag{34}$$

The number of protons ejected during the flare into the interplanetary medium is

$$N_p^\Sigma=\int_S F_p\,dS. \tag{35}$$

Here F_p is the total flux of protons through a 1-cm^2 area throughout the flare.

In the flare of Aug. 4, 1972, the total flux of protons of energy 1–5 MeV at the orbit of the Earth was $\sim2\times10^9$ particles/cm^2. Hence we have

$$N_p^\Sigma(E\geqslant1\text{MeV})\approx10^{37}\frac{\Delta\Omega}{4\pi}\text{ (particles)}, \tag{36}$$

Here $\Delta\Omega$ is the solid angle occupied by the protons ejected in the flare.

If we take the total numbers of protons "settled" in the atmosphere of the Sun N_p^Σ to be equal, we get from (34) and (36):

$$F_\gamma\sim10^3\frac{\Delta\Omega}{4\pi}\text{ (quanta/cm}^2\text{)}. \tag{37}$$

The duration of generation of line γ-rays at 2.2 MeV in the flare of Aug. 4, 1972 was $\Delta t\sim10^3$ sec. Hence the mean flux of γ-quanta of energy 2.2 MeV near the Earth should be $\sim F_\gamma/\Delta t\sim\Delta\Omega/4\pi$ quanta/cm$^2\cdot$ sec. For $\Delta\Omega/4\pi\sim0.1$–1, this quantity is approximately equal to the observed flux of γ-rays of 2.2 MeV, which amounts to 0.28 quanta/cm$^2\cdot$ sec.[49] Consequently we can explain the observed intensity of the given γ-line within the framework of the hypothesis that the 2.2-MeV γ-line is generated by capture of thermal neutrons by protons.

The 4.4 and 6.1 MeV lines amount to emission from excited ^{12}C and ^{16}O nuclei (see Sec. 2). Excitation of ^{12}C and ^{16}O nuclei in a solar-flare region arises mainly from their collision with protons having an energy $\sim$(10–100) MeV. In the γ-emission of the 4.4-MeV line, a substantial contribution also comes from the spallation reaction of oxygen: $^{16}O(p,\alpha p)(^{12}C_{4.43})^*$. Estimates show that excitation of ^{12}C and ^{16}O nuclei requires a total number of accelerated protons in the flare region analogous to the quantity given in Eq. (36).[4]

The 0.5-MeV line is produced by annihilation of positrons with electrons of the photosphere of the Sun. The source of positrons is pions and radioactive nuclei.[50]

The mean energy of the positrons in the decay $\pi^+\to\mu^+\to e^+$ is $\sim70m_ec^2$.[51] The generated ultrarelativistic positrons in the flare region ($n_e\sim10^{10}$–10^{12} cm^{-3}, $H\sim100$–

1000 gauss) at first lose their energy mainly by synchrotron radiation, and then (after slowing down to energies ~1 MeV), ionization losses begin to predominate (for more details, see Sec. 2).

The positrons produced by β-decay of the radioactive nuclei ^{11}C, ^{12}N, ^{13}N, ^{14}O, ^{15}O, etc. have mean energies from hundreds of keV to several MeV and are slowed down by ionization losses.

There is a ~10% probability that a positron will be annihilated while having a relativistic velocity.[44] However, owing to Doppler broadening, this annihilation does not contribute to the intensity of the 0.5-MeV line (see Sec. 2).

The positrons slowed down to nonrelativistic velocities annihilate with electrons of the photosphere of the Sun. Here α-rays are produced of energy 0.5 MeV. Just as in the case of the 4.4- and 6.1-MeV γ-lines, the number of protons in the region of a solar flare required to explain the intensity of the 0.5-MeV line is close to the value given in (36) in order of magnitude.

Line γ-radiation is another information channel concerning solar flares. Observations of the γ-line of quantum energy 0.5 MeV allow one to estimate the plasma parameters in the region of production of this γ-ray line. Namely, analysis of the time-dependence of the intensity of the annihilation line observed during the solar flare of Aug. 4, 1972 implies that the density of matter and the magnetic field intensity in the annihilation region exceed ~10^{12} cm^{-3} and ~500 gauss, respectively.[44] We note that the width of the 0.5-MeV line is very sensitive to the temperature T of the surrounding plasma [see Eq. (31)], and one can determine T by measuring the width of this γ-line. The existing measurements[52] offer only an upper limit on the temperature of the plasma in the annihilation region, which is ~10^7 °K.[4]

However, instruments already in existence (e.g., those using germanium detectors) can measure the width of the 0.5-MeV line to an accuracy of ~1 keV, and hence measure the temperature of the plasma in the region of a flare to an accuracy of ~10^4 °K.

As we have noted, annihilation of positrons can occur either in the free or the bound state (see Sec. 2 and Fig. 6). The probability of producing positronium of spin 0 amounts to 25%, and of spin 1 to 75% (see, e.g., Ref. 50). Positronium in the singlet state has a mean lifetime of 1.2×10^{-10} sec and decays into two quanta of energy 0.51 MeV. Positronium in the triplet state has a mean lifetime of 1.4×10^{-7} sec and decays into three γ-quanta of energy $\leq$0.51 MeV. If the density of the surrounding medium is greater than ~10^{15} cm^{-3}, then triplet positronium is dissociated by electron collisions, and free annihilation plays the major role. The latter also dominates in the case of a rarefied plasma if its temperature exceeds 10^6 °K (see Sec. 2).[4] According to the observational data on the hard x-rays and soft γ-rays of the Sun, the fraction of positrons that undergo three-photon annihilation does not exceed ~20% of the total number of positrons annihilating in the solar atmosphere. Hence, in the region of annihilation of positrons we have either $n_e \gtrsim 10^{15}$ cm^{-3} or $T \gtrsim 10^6$ °K.

TABLE IV

	Model of a thin radiating layer	Model of a thick radiating layer
$He^3/H=0$	2 ± 0.2	3 ± 0.3
$He^3/H=5\cdot10^{-5}$	1.8 ± 0.2	2.7 ± 0.2

Observations of γ-lines allow one to decide on the spectrum of accelerated protons and nuclei of energy ~10 MeV/nucleon directly in the region of a solar flare. This involves the fact that the mean energies of the accelerated particles responsible for generating different γ-lines differ. Consequently we can determine from the measured ratio of γ-line intensities the ratio of densities of particles having different energies, i.e., find the particle spectrum. For example, let us study the 2.2- and 4.4-MeV lines. The ratio of intensities of these lines observed during the flare of Aug. 4, 1972 was $\Phi_{4.4}/\Phi_{2.2}=0.11\pm0.04$. Assuming the spectrum of accelerated particles in the flare region to be the power function of (12), we can determine the exponent of the spectrum (see Sec. 2). Table IV gives the values of the exponent of the proton spectrum under different hypotheses concerning the ratio of concentrations of ^3He and H in the plasma and the nature of the interaction of protons with nuclei.[4]

We note that the value of the exponent of the proton energy spectrum obtained in the thin-layer model $s\approx2$ is close to the exponent of the proton spectrum at energies ~10–100 MeV observed on the day of the flare (Aug. 4, 1972) outside the Earth's atmosphere.

The detection of γ-rays of 2.2-MeV energy in the solar flare of Aug. 4, 1972 showed that an appreciable fraction of the neutrons is not absorbed by helium nuclei. Hence the ratio of concentrations of helium and hydrogen in the subphotospheric layers does not substantially exceed the value of ~5×10^{-5} observed in the plasma of the solar wind.

In closing this section, we emphasize that all these results have been obtained from observing the γ-lines from only one large solar flare. Evidently further studies of solar γ-lines together with simultaneous observations of the continuous radiation over a broad frequency range will allow us to advance considerably in understanding the physics of solar flares.

b) Galactic γ-lines

Galactic γ-lines are produced either by annihilation of positrons with electrons or by emission from excited nuclei of ^7Li, ^{12}C, ^{20}Ne, ^{24}Mg, ^{28}Si, etc. For most of the observed γ-lines we cannot yet finally say whether they originate in discrete sources (pulsars and supernova remnants) or in extended regions upon interaction of subcosmic rays with the interstellar gas.

Table V gives the most probable identifications of the observed galactic γ-lines. For all these identifications, we can explain the observed intensities of the galactic γ-lines by using the formulas of Sec. 2 with an appro-

TABLE V

Energy of observed γ-lines, MeV	Nature of the γ-radiation	Emitting object
0.400±0.001	Emission in annihilation of positrons and electrons	Pulsar NP 0532 in the Crab Nebula
0.476±0.24	1. Emission from excited ^{7}Li nuclei with mean quantum energy 0.478 MeV	a) Interstellar medium. Lithium nuclei contained in cosmic rays are excited on colliding with particles of the interstellar gas.[53] b) Pulsars. The excited lithium nuclei are produced by collisions of helium nuclei emerging from young pulsars with helium nuclei contained in the gaseous shell ejected in formation of the pulsar.[54] Neutron star accreting the surrounding gas.[55]
	2. Emission in annihilation of positrons and electrons	The difference of the mean energy of the detected γ-quanta from 0.511 MeV is due to the red shift of the quantum energy in the powerful gravitational field of the neutron star.
0.53±0.01	Emission in annihilation of positrons and electrons[16]	Interstellar medium. The positrons in the interstellar medium are produced by decay of β-radioactive nuclei, and also by decay of positive pions produced in collisions of cosmic-ray protons with particles of the interstellar gas.
0.9±0.1	Emission from excited ^{56}Fe nuclei with mean quantum energy of 0.847 MeV.[16]	Interstellar medium.
1.2—2	Several unresolved γ-lines.[16] Most likely these lines are generated by excited nuclei of ^{20}Ne, ^{24}Mg, and ^{28}Si	Interstellar medium. Nuclei of Ne, Mg, and Si contained in cosmic rays are excited upon colliding with particles of the interstellar gas.
1.15±0.07	Emission from excited ^{44}Sc nuclei with mean quantum energy 1.156 MeV.[44]	Supernova remnant. The excited ^{44}Sc nuclei are produced by decay of ^{44}Ti created in the explosion of the supernova. The half-life of ^{44}Ti amounts to ~10^3 years.
4.6±0.1	Emission from excited ^{12}C nuclei with mean quantum energy 4.43 MeV.[16]	Interstellar medium. Carbon nuclei contained in cosmic rays are excited upon colliding with particles of the interstellar gas.

priate choice of parameters (density of the interstellar medium, density of subcosmic rays, flux of particles from a pulsar, etc.) that do not contradict any other observational data. Now we shall discuss in greater detail only the nature of the 0.4-MeV γ-line from the Crab Nebula, which is a remnant from the explosion of the supernova of 1054. Most probably this radiation arises from e^+e^- annihilation at the surface of the pulsar NP 0532, which lies inside the Crab Nebula. We can explain in a natural manner the difference of the mean energy of the detected γ-quanta from 0.511 MeV by a gravitational red shift with $z=(0.511-0.400)/0.400=0.28$. This is the size of red shift that should arise as quanta emerge from the surface of a neutron star of mass ~$1.4M$. In order to explain the luminosity $L_\gamma \sim 4\times10^{35}$ erg/sec of pulsar NP 0532 in the given γ-line, we must assume that $L_\gamma/2m_ec^2 \sim 10^{41}$ positrons are annihilated at its surface per second. Interestingly, about the same number of electrons (and perhaps of positrons) must be ejected from pulsar NP 0532 into the Crab Nebula to maintain its luminosity at the observed level.[56]

Essential information on the region of generation of the 0.4-MeV γ-line is given by measurements of the line width ΔE_γ: $\Delta E_\gamma \lesssim 3$ keV. This implies that the radial dimension of the region of production of the 0.5-MeV line at the surface of the pulsar is

$$\Delta R \ll \frac{\Delta E_\gamma}{E_\gamma} R \sim 10^4 \text{ cm}.$$

Here $R \sim 10^6$ cm is the radius of the neutron star. The nature of the source of such a large number of positrons near the surface of pulsar NP 0532 has not been finally established. We can only say that these positions are not in thermodynamic equilibrium with the surrounding plasma, since otherwise the plasma should have a temperature higher than ~10^8 °K, while this does not agree with $\Delta E_\gamma \lesssim 3$ keV [see Eq. (31)].

c) γ-lines from the radiogalaxy Cen A

Cen A is the radiogalaxy nearest to us, which coincides with the optical galaxy NGC 5128. The distance to Cen A is about 5 megaparsecs. Two gigantic radio clouds are observed on opposite sides of the optical galaxy NGC 5128. The emission from these clouds is generated by relativistic electrons moving in a magnetic field (synchrotron radiation). These radio-emitting clouds were produced either by explosion of the core of the galaxy NGC 5128 or by quasistationary ejection from it of relativistic electrons. The high-power processes in the radiogalaxy Cen A have not only occurred in the past but continue into the present. This is indicated by observations from it of infrared radiation x-rays, and γ-rays, which are apparently nonthermal in origin. Hence it is quite natural to detect powerful γ-radiation from Cen A in the 1.6 and 4.5 MeV lines.

Most likely, the broad γ-line of mean quantum energy 1.6 MeV amounts to the total γ-radiation of excited nuclei of ^{20}Ne, ^{24}Mg, and ^{28}Si, whose γ-line energies lie very close and are as yet unresolved. Apparently the γ-line at 4.5 MeV is emitted by excited ^{12}C nuclei. Let us estimate the parameters that would allow us to understand, e.g., the intensity of the 4.5-MeV γ-line observed from it. In order to do this, we shall employ the following expression for the flux of γ-rays from ^{12}C nuclei in the 4.43-MeV line (see Ref. 16):

$$F_\gamma = \frac{V n_p \Phi_c P}{4\pi r^2}. \tag{38}$$

Here V is the volume of the region of generation of the 4.43-MeV γ-line, n_p is the concentration of protons in the interstellar medium inside Cen A, Φ_c is the differential flux of carbon nuclei in the subcosmic rays of Cen A, and P is the differential yield of the nuclear reaction, which is ~4.2×10^{-24} cm$^2\cdot$MeV.[58] For $F_\gamma = 10^{-3}$ quanta/cm$^2\cdot$sec and $r=5$ megaparsecs, we obtain from (38):

$$V n_p \Phi_c \approx 0.6\cdot10^{73} \text{ cm}^{-2}\,\text{sec}^{-1}(\text{MeV/nucleon})^{-1}. \tag{39}$$

When $n_p \sim 1$–10 cm^{-3} and $V \sim 10^{67}$–10^{68} cm^3, we have $\Phi_c \sim 10^3$–10^5 nuclei/cm$^2\cdot$sec (MeV/nucleon). This value of the flux of carbon nuclei in the subcosmic rays of Cen A is about 10^2–10^4 times as great as in our Galaxy. Such a high density of cosmic rays in Cen A is quite natural, since radiogalaxies, including Cen A, are among the most active astronomical objects in the Universe.

6. RESULTS AND FUTURE PROSPECTS

Cosmic γ-spectroscopy is a young research field. The first γ-lines of cosmic origin[2)] were discovered

[2)] In this review we are not treating γ-lines of planetary origin (for more details, see the monograph of Ref. 58).

only several years ago in observations of the high-power solar flare in August 1972. In the following five years γ-lines have been detected from the galactic center, from the pulsar NP 0532 in the Crab Nebula, and from the radiogalaxy Cen A. There are also indications of γ-ray lines in other regions of the celestial sphere. It is worth noting that the radiation flux in these lines lies at the limit of sensitivity of modern γ-spectrometers and does not substantially exceed 3–4 standard deviations. Perhaps subsequent studies will not confirm some of the published results on detection of cosmic γ-lines. However, the reliability of the observations of most of the cosmic γ-lines gives no cause for doubt.

In spite of the small number of objects from which γ-lines have been detected and the small number of observed γ-lines, cosmic γ-spectroscopy has already substantially deepened our concepts of certain astrophysical phenomena. Thus, for example, observations of γ-lines allow us:

1) to make conjectures, although to date only crude ones, concerning the parameters of the regions of solar flares (magnetic field intensity, plasma concentration and temperature);

2) to estimate the exponent of the spectrum of accelerated protons immediately in the region of a solar flare;

3) to "weigh" the pulsar NP 0532 that lies inside the Crab Nebula and is genetically associated with it;

4) to estimate the density of subcosmic rays in our Galaxy and in the radiogalaxy Cen A.

The list of the most urgent problems of cosmic γ-spectroscopy includes:

1. To confirm the existence of the observed γ-lines and to seek new γ-lines from nonstationary astronomical objects.

2. To perform simultaneous observations of a large number of γ-lines, since only this type of measurements will allow us to solve many astrophysical problems (e.g., to determine the spectrum and chemical composition of cosmic rays in the region of generation of the γ-lines, and also to form opinions concerning the parameters of the thermal plasma in this region).

3. To measure the angular paremters, and if possible, to study the structure of the γ-line source by increasing the angular resolution of γ-spectrometers. This will substantially facilitate the identification of γ-line sources.

4. To study in detail the shape of the γ-lines. This is possible when one uses Ge (Li) spectrometers. We can estimate more reliably the parameters of the emitting region of cosmic objects (e.g., the plasma temperature) by reducing the instrumental width of the lines to a minimum.

Perhaps in the future the recent discovery of baryonium (a bound state of a nucleon and an antinucleon[59,60]) will be of great importance in determining the concentration of matter in the Universe. This system, which is named by analogy with positronium, can have excited levels with a transition energy $E_\gamma \sim 100$–1000 MeV.

In closing this article we wish to note that cosmic γ-spectroscopy undoubtedly has a great future, since observations of cosmic γ-lines are apparently the only information channel on the characteristics of the nuclear component of subcosmic rays inside various astronomical objects.

Note added in proof. A symposium was held on Apr. 28–29, 1978 in the United States on cosmic γ-spectroscopy. A short account of the proceedings of the symposium is given in an article by R. Ramaty *et al.* [Nature **273**, 591 (1978)]. The account indicates that γ-ray lines with E_γ of 0.511 and 4.4 MeV from the galactic center have been confirmed. The half-width of the 0.511-MeV γ-line proved to be very small ($\Delta E_\gamma \lesssim 3$ keV). There are also indications of existence in the γ-ray spectrum of the galactic center of an excess caused by three-photon annihilation of positrons.

[1]A. M. Gal'per, V. G. Kirillov-Ugryumov, B. I. Luchkov, and O. F. Prilutskiĭ, Usp. Fiz. Nauk **105**, 207 (1971) [Sov. Phys. Usp. **14**, 630 (1972)].
[2]Yu. M. Goryachev, V. P. Kanavets, I. V. Kirpichnikov, and I. I. Levintov, Yad. Fiz. **17**, 910 (1973) [Sov. J. Nucl. Phys. **17**, 476 (1973)].
[3]B. M. Kuzhevskiĭ, Astron. Zh. **45**, 747 (1968) [Sov. Astron. **12**, 595 (1969)].
[4]R. Ramaty and R. E. Lingenfelter, Proceedings of the 6th Leningrad International Seminar, LIYaF AN SSSR, L., 1974.
[5]B. Kozlovsky and R. Ramaty, Astrophys. J. **191**, L43 (1974).
[6]N. A. Roughton, M. J. Fritts, R. J. Peterson, C. S. Zaidins, and C. J. Hansen, *ibid.* **188**, 595 (1974).
[7]N. A. Roughton, M. J. Fritts, R. J. Peterson, C. S. Zaidins, and C. J. Hansen, *ibid.* **193**, 187 (1974).
[8]R. Lingenfelter, in Proc. Internat. Symposium Structure Galaxy and Galactic γ-Rays, Greenbelt, 1976, p. 164.
[9]Y. W. Truran, Astrophys. and Space Sci. **18**, 306 (1972).
[10]I. L. Rosental'. Usp. Fiz. Nauk **121**, 319 (1977) [Sov. Phys. Usp. **20**, 167 (1977)].
[11]V. L. Ginzburg and S. I. Syrovatskiĭ, *Proiskhozhdenie kosmicheskikh luchei* (The Origin of Cosmic Rays), Izd-vo AN SSSR, M., 1963 (Engl. Transl., Pergamon Press, Oxford-New York, 1964).
[12]M. Leventhal, Astrophys. J. **183**, L147 (1973).
[13]F. W. Stecker, *Cosmic Gamma Rays*, NASA, Washington, 1971.
[14]W. Heitler, *The Quantum Theory of Radiation*, 3rd Edn., Clarendon Press, Oxford, 1954 (Russ. Transl., IL, M., 1956).
[15]J. L. Trombka, A. E. Metzger, J. R. Arnold, J. L. Matteson, R. C. Reedy, and L. E. Peterson, Astrophys. J. **181**, 737 (1973).
[16]R. C. Haymes, G. D. Walraven, C. A. Meegan, R. D. Hall, F. T. Djuth, and D. H. Shelton, *ibid.* **201**, 593 (1975).
[17]L. S. Peterson, J. Geophys. Res. **68**, 979 (1963).
[18]A. E. Metzger, E. C. Anderson, M. A. Van Dilla, and J. R. Arnold, Nature **204**, 766 (1964).
[19]B. P. Konstantinov, M. M. Bredov, A. I. Belyavskiĭ, and I. A. Sokolov, Kosm. Issled. **4**, 66 (1966).
[20]E. L. Chupp, P. J. Lavakare, and A. A. Sarkady, Phys. Rev. **166**, 1297 (1968).
[21]E. P. Mazets, S. V. Golenetskiĭ, and V. N. Il'inskiĭ, Pis'ma Astron. Zh. **2**, 563 (1976) [Sov. Astron. Lett. **2**, 223 (1976)].
[22]I. V. Êstulin, in *Issledovanie kosmicheskikh luchei* (Study of Cosmic Rays), Nauka, M., 1975, p. 67.

[23]I. V. Éstulin and V. P. Ivanov, Kosm. Issled. **11**, 956 (1973).
[24]E. L. Chupp, D. J. Forrest, P. R. Higbie, A. N. Suri, C. Tsai, and P. P. Dunphy, Nature **241**, 333 (1973).
[25]P. R. Higbie, E. L. Chupp, S. Y. Forrest, and I. U. Cleske, IEEE Trans. Nucl. Sci. **NS-19**, 606 (1972).
[26]G. D. Walraven, R. D. Hall, C. A. Meegan, P. L. Coleman, D. H. Shelton, and R. C. Haymes, Astrophys. J. **202**, 502 (1975).
[27]G. H. Nakano, W. L. Imhof, and R. G. Johnson, IEEE Trans. Nucl. Sci. **NS-21**, 159 (1974).
[28]W. L. Imhof, G. H. Nakano, and J. B. Reagan, J. Geophys. Res. **81**, 2835 (1976).
[29]W. L. Imhof and G. H. Nakano, Astrophys. J. **214**, 38 (1977).
[30]E. A. Womack and J. W. Overrbeck, J. Geophys. Res. and Space Phys. **75**, 1811 (1970).
[31]F. Albernhe and G. Vedrenne, J. Geophys. Res. **81**, 2433 (1976).
[32]N. L. Grigorov, O. M. Kovrizhnykh, and M. I. Kudryavtsev, Solnechnye Dannye **1973**, No. 6, 95.
[33]A. N. Suri, E. L. Chupp, D. J. Forrest, and C. Reppin, Solar Phys. **43**, 415 (1975).
[34]G. Kanback, C. Reppin, D. J. Forrest, and E. L. Chupp, Proc. 14th Intern. Cosmic Ray Conference, München, 1975, Vol. 5, p. 1944.
[35]R. Talon, G. Vedrenne, A. C. Melioransky, N. F. Pissarenko, V. N. Shamolin, and O. B. Likin, Internat. Astronomical Union Symposium No. 68, D. Reidel, Dordrecht, Holland; Boston, USA.
[36]W. N. Johnson III, F. R. Harnden, Jr., and R. C. Haymes, Astrophys. J. **172**, L1 (1972).
[37]W. N. Johnson III and R. C. Haymes, Astrophys. J. **184**, 103 (1973).
[38]G. D. Walraven, R. D. Hall, C. A. Meegan, P. L. Coleman, D. H. Shelton, and R. C. Haymes, Astrophys. J. **202**, 502 (1975).
[39]R. D. Hall, C. A. Meegan, G. D. Walraven, F. T. Djuth, and R. C. Haymes, Astrophys. J. **210**, 631 (1976).
[40]G. D. Walraven and R. C. Haymes, Nature **264**, 42 (1976).
[41]M. Leventhal, C. J. MacCallum. and A. C. Watts, Nature **266**, 696 (1977).
[42]R. E. Lingenfelter and R. Ramaty, Internat. Gamma-Ray Symposium, Goddard Space Flight Center, June 2–4, 1976.
[43]A. S. Jacobson, J. B. Willett, W. A. Mahoney, and J. C. Ling, Bull. Am. Astron. Soc. **8**, 528 (1976).
[44]H. T. Wang and R. Ramaty, Astrophys. J. **202**, 532 (1975).
[45]H. T. Wang and R. Ramaty, Solar Phys. **36**, 129 (1974).
[46]H. T. Wang and R. Ramaty, see Ref. 34.
[47]B. M. Kuzhevskiĭ, Pis'ma Astron. J. **2**, 581 (1976) [Sov. Astron. Lett. **2**, 230 (1976)].
[48]G. M. Blokh and B. M. Kuzhevskiĭ, see Ref. 22.
[49]A. H. Suri, E. L. Chupp, D. J. Forrest, and C. Reppin, Solar Phys. **43**, 415 (1975).
[50]I. A. Ibragimov and G. E. Kocharov, Izv. Akad. Nauk SSSR Ser. Fiz. **41**, 327 (1977).
[51]R. E. Lingenfelter and R. Ramaty, in *High Energy Reactions in Astrophysics*, Ed. W. Shen, W. Benjamin, New York, 1967.
[52]E. L. Chupp, Invited paper presented at the IAU/COSPAR Symposium No. 68 on Solar *X*- and EUV Radiations, Buenos Aires, June 11–14, 1974.
[53]G. J. Fishman and D. D. Clayton, Astrophys. J. **178**, 337 (1972).
[54]D. D. Clayton and E. Dwek, *ibid.* **206**, L59 (1976).
[55]R. Ramaty, G. Borner, and J. M. Cohen, Astrophys. J. **181**, 891 (1973).
[56]I. S. Shkovsky, *ibid.* **159**, L77 (1970).
[57]T. A. Rygg and G. J. Fishman, Proc. 13th Internat. Cosmic Ray Conference, Denver, 1973, Vol. 1, p. 472.
[58]Yu. A. Surkov, *Gamma-spektroskopiya v kosmicheskikh issledovaniyakh* (Gamma Spectroscopy in Space Research), Atomizdat, M., 1977.
[59]I. S. Shapiro, Usp. Fiz. Nauk **118**, 740 (1976) [Sov. Phys. Usp. **19**, 356 (1976)].
[60]CERN Courier **17**, 71 (1977).

Translated by M. V. King